ELSEVIER

Catalysis Today 78 (2003) 513–518

CATALYSIS TODAY

www.elsevier.com/locate/cattod

Niobium sulfide as a dopant for Mo/TiO_2 catalysts

Luis Cedeño Caero [a,b,*], Alma R. Romero [a,b], Jorge Ramirez [a]

[a] *UNICAT, Facultad de Quimica, UNAM, Mexico D.F. 04510, Mexico*
[b] *Instituto Mexicano del Petroleo, Mexico D.F. 07730, Mexico*

Abstract

Mo/TiO_2 catalysts were modified with Nb by two different methods, sol–gel and surface deposition, in order to study the effect of Nb incorporation on the thiophene HDS activity. The results show that the formation of Nb–Ti mixed oxides leads to catalysts with poor HDS activity while the deposition of Nb oxide species on the surface of TiO_2 leads to catalysts with activities larger than those of Mo/Al_2O_3 and Mo/TiO_2. This increase in activity was attributed to the formation of a larger population of Mo sulfur anionic vacancies when Nb was surface deposited on the TiO_2.

Keywords: Hydrodesulfurization; Mo/TiO_2 catalysts; Niobium; TPR

1. Introduction

Hydrotreating catalysts are usually supported on acidic supports such as alumina. However, the need for more active and/or selective hydrotreating catalysts has induced research on the use of not only new active phases but of new catalytic supports with the purpose of enhancing one or some of the catalyst functionalities, according to the petroleum cut to be processed. For example, it has been established that Mo-based hydrodesulfurization (HDS) catalysts supported on TiO_2 are several times more active than those supported on alumina. This result has been associated to the redox and semiconductor properties of TiO_2 that help the sulfidation and reduction of the Mo oxide precursors [1].

Among the new catalytic phases proposed to obtain more active HDS catalysts, the use of niobium sulfide has attracted attention. Previous reports indicate that in the unsupported state, niobium sulfide exhibits unique acidic properties [2], and when supported on carbon or alumina it is possible to obtain catalytic activities in HDS higher than those of a MoS_2/Al_2O_3 catalyst with equivalent metal loading [3,4]. It has been demonstrated that the nature of the niobium precursor salt and the support also influence the HDS activity and the difficulty of sulfidation of the catalyst. Moreover, the addition of niobia as promoter to the typical hydroprocessing catalysts resulted in an increase of the HDS and HDN activities [5].

In the present work, we analyze the effect that the incorporation of small amounts of Nb to MoS_2/TiO_2 catalysts by different methods causes on their HDS activity. Two different routes were used to incorporate niobium to the catalyst support in order to produce a Ti–Nb mixed oxide, or a TiO_2 covered with niobium oxide. The catalysts were characterized by pyridine adsorption analyzed by FT-IR and by temperature programmed reduction of the oxide and sulfided samples, before and after catalytic test. The catalysts were tested in the thiophene HDS reaction.

* Corresponding author. Present address: UNICAT, Facultad de Quimica, UNAM, Mexico D.F. 04510, Mexico.
E-mail address: lcedeno@imp.mx (L. Cedeño Caero).

0920-5861/02/$ – see front matter
PII: S0920-5861(02)00342-5

2. Experimental

2.1. Supports and catalysts preparations

The Nb–TiO_2 mixed oxides were prepared by the simultaneous hydrolysis of Ti isopropoxide and Nb ethoxide, followed by drying (373 K, 24 h) and calcination (773 K, 4 h). The niobium-covered samples, Nb/TiO_2, were prepared by pore volume impregnation of TiO_2 (Degussa P-25, 74 m^2/g) with niobium ethoxide followed by hydrolysis in wet air. The Nb–TiO_2 and Nb/TiO_2 samples were prepared with Nb contents of 2, 4 and 6 wt.%.

The deposition of Mo on the calcined supports was also achieved by pore volume impregnation using an aqueous solution of ammonium heptamolybdate. The catalysts were dried at 100 °C during 24 h and calcined at 500 °C (4 h). As reference, two additional samples were prepared by similar methods, molybdenum supported on alumina (Gilder, 180 m^2/g), Mo/Al_2O_3, and molybdenum supported on alumina covered with niobium oxide (4 wt.% as Nb), Mo/Nb/Al_2O_3.

2.2. Characterization and catalytic test

The supports were characterized by several techniques. X-ray diffraction (XRD) patterns were recorded using a Siemens D500 powder diffractometer with Cu Kα radiation. Surface areas and N_2 adsorption–desorption isotherms of the samples were measured with an ASAP 2000 Micromeritics apparatus. The FT-Raman spectra of supports were taken in a Nicolet FT-Raman 950. The samples were pretreated at 373 K during 12 h in static air before taking the spectrum.

A conventional TPR apparatus with TCD and UV detectors was used for the study of the reducibility of calcined and sulfided (TPR-S) catalysts. The sulfided catalysts were analyzed by TPR-S before and after the reaction test, as described previously [1]. Before the catalytic test, the samples were sulfided at 673 K for 4 h using a stream of H_2S–H_2 (15% H_2S (v/v)). The catalytic activity tests for thiophene HDS, at 623 and 673 K, were carried out at atmospheric pressure in a typical continuos differential micro-reactor apparatus. All the activity tests were made with the same total amount of catalyst (0.25 g). Reactant and product analysis was performed with a gas chromatograph equipped with a FID detector and an Ultra-I 30 m. column. The thiophene HDS activity of sulfided catalysts was determined at 623 and 673 K.

The acid properties of the samples were obtained from the analysis of the IR spectra of adsorbed pyridine. The adsorption of pyridine was performed using a special IR cell connected to a high vacuum line and a gas-manipulating manifold. Before pyridine adsorption at room temperature (RT), the catalysts were pretreated under a flow of oxygen at 673 K during 20 h, followed by evacuation (2 h) and cooling to RT. The IR spectra of the samples were taken, at RT, 423, 523 and 623 K, after evacuation during 30 min.

3. Results and discussion

3.1. Supports selection of the Mo catalysts

The results from the textural characterization, for the Nb(wt.%)–TiO_2 mixed oxides and titania covered with niobium oxide (Nb(wt.%)/TiO_2), are shown in Table 1. All the samples exhibit textural properties similar to those of the reference commercial and synthesized titania. This indicates that the incorporation of small amounts of niobium do not alter significantly the textural properties of the original corresponding titania support.

The structural characterization by XRD and FT-Raman show only the presence of anatase phase, indicating a reasonably good dispersion of the Nb phases in all cases. Because of these minor differences only the samples with 4 wt.% Nb prepared by the two methods were evaluated in the activity tests and characterized further to explain the observed differences in HDS catalytic activity. Thus, the part of the work

Table 1
Results of N_2 adsorption measurements

	Surface area (m^2/g)	Pore volume (cm^3/g)	Average pore diameter (Å)
Nb(6%)–TiO_2	125	0.12	38
Nb(4%)–TiO_2	132	0.13	40
Nb(2%)–TiO_2	114	0.10	37
TiO_2 (synthesized)	115	0.11	39
Nb(6%)/TiO_2	78	0.28	145
Nb(4%)/TiO_2	70	0.27	151
Nb(2%)/TiO_2	71	0.28	155
TiO_2 (commercial)	74	0.30	161

that follows will be centered in the comparison of the two methods of preparation using a fixed amount of niobium (4 wt.%) incorporated to the catalysts. This proposal is in line with the previous finding that around 5 wt.% Nb incorporated to $NiMo/Al_2O_3$ catalysts yielded the maximum activity in the HDS of dibenzothiophene [5] and gasoil [6].

3.2. Surface acidity

It is well known that surface acidity plays a role in hydrotreating reaction mechanisms. In fact, changes in surface acidity are a consequence of the nature of the surface species present in the catalyst. Regarding hydrotreating reactions direct correlation between catalyst acidity, in the sulfided, oxide or reduced state of the catalyst, and the desulfurization and denitrogenation activities has been observed [7,8]. Regarding niobium-modified $NiMo/Al_2O_3$ catalysts, it has been found that the maximum in HDS and HDN of gasoil, corresponds with the highest acidity of the catalysts [6].

Acidity results from the quantitative analysis of the IR spectra of pyridine adsorbed in our samples, are shown in Table 2. The concentration of the Lewis and Brönsted acid sites, calculated from the intensity of the 1450 and 1540 cm^{-1} bands, respectively, are shown in Table 2. Two important results were obtained: (i) the incorporation of Mo promoted the formation of Brönsted acid sites without altering in the same proportion the total number of acid sites. This indicates that part of the original Lewis sites present in the support are suppressed by the deposition of Mo while the Mo species provides additional Brönsted sites. This is clearly evidenced in the case of Mo supported on Nb/TiO_2 since in this sample the Brönsted acid sites were created only after the incorporation of Mo; (ii) when Nb is incorporated to titania, the acidity changes depend of the preparation method. For titania covered with Nb, no Brönsted sites are detected while in the $Nb–TiO_2$ mixed oxide the presence of Brönsted sites is clearly evident.

3.3. Temperature programmed reduction

3.3.1. Oxide samples

Fig. 1 shows the TPR profiles of the oxide catalysts. For comparison, the TPR of Mo/Al_2O_3 and $Mo/Nb/Al_2O_3$ are also included in the figure. $Mo/Nb/TiO_2$ and $Mo/Nb–TiO_2$ samples show in general the same reduction peaks than those observed in the Mo/Al_2O_3 and $Mo/Nb/Al_2O_3$. A low temperature peak ($T \approx 723$ K) assigned to the presence of octahedral well dispersed Mo species and a high temperature peak, which contains contributions from the second step reduction of octahedral Mo species and from the reduction of tetrahedral Mo species, in strong interaction with the support. In between these two peaks there is a reduction zone at intermediate temperatures that contains contributions from the reduction of octahedral Mo species with different degrees of polymerization including segregated bulk MoO_3. However, there are clear differences between the two samples under study ($Mo/Nb/TiO_2$ and $Mo/Nb–TiO_2$). It is clear that in the $Mo/Nb/TiO_2$ sample there is a higher proportion of polymeric octahedral Mo species and that there is only a small amount of tetrahedral Mo species in strong interaction with the support, which are known to be difficult to reduce and sulfide. In contrast, the $Mo/Nb–TiO_2$ sample presents a high consumption of hydrogen and a very pronounced high temperature peak which contains the contribution from an apparently large population of tetrahedral Mo species in strong interaction with the support. This

Table 2
Lewis (L) and Bronsted (B) acid sites concentration as function of desorption temperature[a]

T (K)	Mo/TiO_2 (1)		$Mo/Nb/TiO_2$		Nb/TiO_2		Mo/TiO_2 (2)		$Mo/Nb–TiO_2$		$Nb–TiO_2$	
	L	B	L	B	L	B	L	B	L	B	L	B
300	246	60	129	141	305	0	85	144	150	160	210	76
423	140	51	64	129	191	0	71	116	115	147	170	72
523	127	31	62	122	170	0	51	68	64	142	155	55
623	120	28	58	99	155	0	43	38	48	85	134	46

[a] Mo on commercial (1) and synthesized (2) titania.

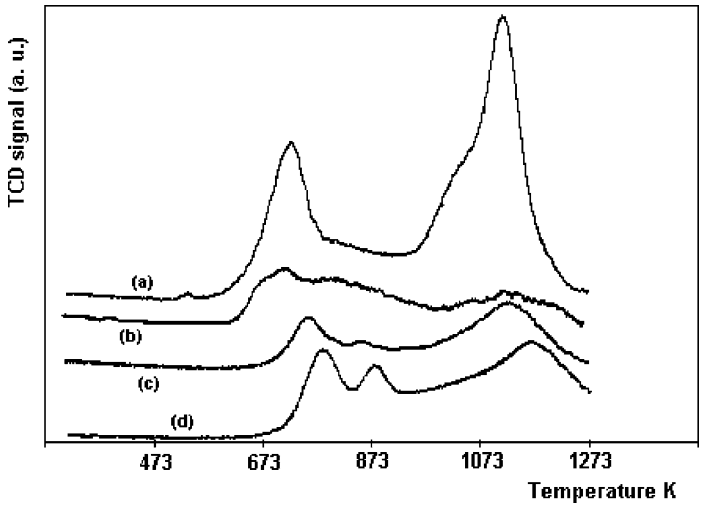

Fig. 1. TPR patterns of the oxide catalysts: (a) Mo/Nb–TiO_2; (b) Mo/Nb/TiO_2; (c) Mo/Al_2O_3; (d) Mo/Nb/Al_2O_3 catalysts.

clearly indicates a high dispersion of the Mo species on the Nb–TiO_2 mixed oxide support. The shoulder on the low temperature side of this high temperature peak is related to the reduction second step of the octahedral well dispersed Mo species of which their first reduction step is the low temperature peak that appears at around 723 K. Therefore, the manner in which the Nb is incorporated to TiO_2, affects drastically the reducibility of the Mo supported species (higher H_2 consumption for the Mo/Nb–TiO_2 catalyst), and the relative population of tetrahedral and octahedral Mo species in the catalyst.

The formation of segregated MoO_3 particles on the Ti-containing supports, evidenced by a reduction peak at 873 K [9,10], is clear from the comparison of the different TPR traces. This does not occur for the alumina-containing supports where the peak related to the reduction of MoO_3 particles is very clear. The TPR of the supports Nb/TiO_2 and Nb–TiO_2 (not shown), put in evidence a small hydrogen consumption at about 670 K, which would overlap with the first reduction of octahedral Mo.

3.3.2. Sulfided samples

Fig. 2 presents the H_2S evolution profiles obtained during TPR of the sulfided catalysts before and after reaction. All the samples exhibit a more or less sharp peak at low reduction temperature in the region 373–573 K, a broad small continuous H_2 consumption and H_2S evolution over a broad temperature region, in which small shoulders or a clear peak were developed in some cases. The high temperature peak, which is easily observed in the Mo/Nb–TiO_2, has been assigned in the past to the reduction of stoichiometric sulfur from supported MoS_2-like species [11–13].

The low temperature peak of H_2S evolution, which is related to a similar peak of hydrogen consumption, has been ascribed to the reduction of nonstoichiometric sulfur species (S*x*), adsorbed on coordinatively unsaturated Mo sites. Our results indicate that the

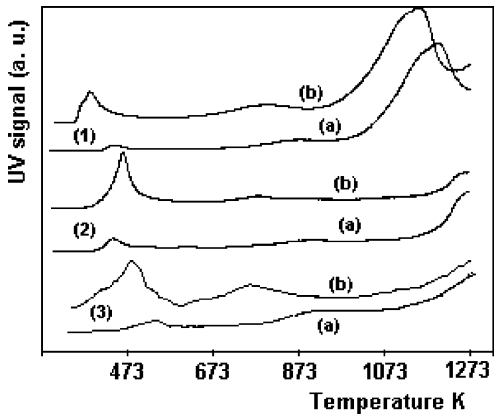

Fig. 2. TPR patterns of the sulfided catalysts (TPR-S), UV signal: (1) Mo/Nb–TiO_2; (2) Mo/Nb/TiO_2; (3) Mo/Al_2O_3 catalysts after (a) and before (b) reaction test.

hydrogen consumed in this region is larger than the H_2S evolution, indicating an extra hydrogen adsorption. A similar result has been already observed in the TPR of sulfided Mo/Al_2O_3 catalysts [14,15].

The TPR traces before and after the catalytic test for the $Mo/Nb/TiO_2$ and $Mo/Nb–TiO_2$ catalysts show clearly that in the former catalyst more sulfur anionic vacancies, which arise from nonstoichiometric sulfur adsorbed on Mo coordinatively unsaturated sites (CUS), are created during TPR. This result that would suggest a higher catalytic activity for the $Mo/Nb/TiO_2$ catalyst, seems to be in contradiction with the TPR of oxided samples, where it was observed a greater reduction degree for the $Mo/Nb–TiO_2$ sample. In fact this result can be rationalized by recalling that the high population of tetrahedral Mo species in interaction with the support, which are in high proportion in the $Mo/Nb–TiO_2$ catalyst, that can be reduced at the conditions of TPR (473–1273 K) but cannot be completely sulfided at the catalyst activation conditions (673 K).

3.4. Catalytic activity

The catalytic activities of the different catalyst formulations in the thiophene HDS are presented in Table 3. For comparison, the results from a Mo/Al_2O_3 and Mo/TiO_2 catalysts have also been included.

As expected, the HDS activity of the Mo/TiO_2 catalyst is greater than for Mo/Al_2O_3. Comparison of the activities of the $Mo/Nb/TiO_2$ and Mo/Nb–Ti catalysts indicate clearly that the effect of adding Nb to the titania support depends on the method of Nb incorporation. The sample $Mo/Nb–TiO_2$ in which the Nb was incorporated trough a sol–gel method leading to a Ti–Nb mixed oxide, and where Nb is present as isolated species forming Ti–O–Nb–O–Ti bonds, exhibited an activity three times smaller than the $Mo/Nb/TiO_2$ sample, in which the Nb was deposited on the surface of TiO_2, leading to the formation of more polymerized Nb oxide species. These results are perfectly consistent with the quantification of the H_2S evolution in the 300–673 K temperature region of the TPR of sulfided samples. As mentioned before, this H_2S evolution is directly related to the concentration of anionic sulfur vacancies in the active MoS_2 phase. A comparison between promoted and unpromoted catalysts is not straightforward and is not attempted because Nb ant Ti species can be reduced and sulfided and can form, under TPR conditions, some sulfur vacancies with very different HDS activity.

Table 3
Thiophene HDS activity ($\times 10^{10}$ mole/m^2 s) and TPR-S results

	HDS activity		H_2S evolution in temperature region 300–673 K (mmole of H_2S)
	673 K	623 K	
Mo/Al_2O_3	24.72	15.51	2.00
Mo/TiO_2	65.86	33.62	n.d.
$Mo/Nb–TiO_2$	36.71	18.32	0.91
$Mo/Nb/TiO_2$	103.64	55.80	2.50

No direct relationship was found between the acidity of the catalysts and the catalytic activity. This could well be due to the fact that the transformation of thiophene occurs by a direct desulfurization route and is not affected by the level of acidity of the catalyst. This, as the literature indicates [6], is not the case for heavier feeds where the acidity enhances the HDS activity.

4. Conclusions

From the above results the following conclusions can be drawn: the way by which Nb is incorporated to the Mo/TiO_2 catalyst support affects significantly the HDS catalytic activity; incorporation through a sol–gel route leads to catalysts with poor HDS activity, while the deposition of Nb on the surface of TiO_2 seems to promote the activity of the MoS_2 active phase, possibly by facilitating the creation of a larger population of Mo sulfur anionic vacancies, believed to be the HDS active sites.

The method of Nb incorporation also affects the acid sites distribution in the catalyst support. Brönsted sites are detected in the $Nb–TiO_2$ support while they are absent in the Nb/TiO_2 case.

Acknowledgements

Experimental assistance of Rogelio Cuevas is gratefully acknowledged. The authors are also grateful to IMP for the financial support through the IMP-FIES program and the sabbatical year of L. Cedeño.

References

[1] J. Ramirez, L. Cedeño, G. Busca, J. Catal. 184 (1) (1999) 59.
[2] M. Danot, J. Alfonso, J.L. Portefaix, M. Breysse, T. des Courieres, Catal. Today 10 (1991) 629.
[3] N. Allali, A.M. Marie, M. Danot, C. Geantet, M. Breysse, J. Catal. 156 (1995) 279.
[4] C. Geantet, J. Alfonso, M. Breysse, N. Allali, M. Danot, Catal. Today 28 (1996) 23.
[5] V. Gaborit, N. Allali, C. Geantet, M. Breysse, M. Vrinat, M. Danot, Catal. Today 57 (2000) 267.
[6] J.G. Weissman, Catal. Today 28 (1996) 159.
[7] S. Rajagopal, T.L. Grimm, D.J. Collins, R. Miranda, J. Catal. 137 (1992) 453.
[8] N.Y. Topsoe, H. Topsoe, J. Catal. 139 (1993) 641.
[9] R. López Cordero, F.J. Gil Llambías, A. López Agudo, Appl. Catal. 74 (1991) 125.
[10] R. López Cordero, L. López Guerra, J.L.G. Fierro, A. López Agudo, J. Catal. 132 (1991) 498.
[11] B. Scheffer, N.J.J. Dekker, P.J. Mangnus, J.A. Moulijn, J. Catal. 121 (1990) 31.
[12] P.J. Mangnus, A. Bos, J.A. Moulijn, J. Catal. 146 (1994) 437.
[13] P.J. Mangnus, A. Riezebos, A.D. Van Langeveld, J.A. Moulijn, J. Catal. 151 (1995) 178.
[14] J. Polz, H. Zeilinger, B. Muller, H. Knözinger, J. Catal. 120 (1989) 22.
[15] L. Jalowiecki, J. Grimblot, J.B. Bonnelle, J. Catal. 126 (1990) 101.